Biosensors and Bioelectronics 141 (2019) 111433

Contents lists available at ScienceDirect

Biosensors and Bioelectronics

journal homepage: www.elsevier.com/locate/bios

Application of metal-organic framework as redox probe in an electrochemical aptasensor for sensitive detection of MUC1

Zahra Hatami, Fahimeh Jalali*, Mahmoud Amouzadeh Tabrizi, Mojtaba Shamsipur

Department of Chemistry, Razi University, Kermanshah, Iran

ARTICLE INFO

Keywords:
MUC1
Electrochemical aptasensor
Metal-organic framework
Reduced graphene oxide

ABSTRACT

In this work, an electrochemical aptasensor was developed for sensitive detection of MUC1 based on metal-organic framework-reduced graphene oxide nanocomposite (Cu-MOF-RGO). Cu- MOF-RGO appeared to be suitable as a platform for immobilization of MUC1 aptamer, and also as an electrochemical probe, which exhibited well-defined peaks with good stability and reproducibility. Cu-MOF-graphene oxide (Cu-MOF-GO) nanocomposite was prepared and cast on the electrode surface, then in order to increase the conductivity of the electrode, GO was electrochemically reduced to RGO. In the presence of MUC1, the peak current of Cu in the nanocomposite decreased, which could be explained based on the formation of MUC1–aptamer complexes on the electrode, and consequence blocking the electron transfer of Cu at the electrode surface. Under optimum experimental conditions, a linear calibration curve was obtained by differential pulse voltammetry in the concentration range of 0.1 pM–10 nM (25 pg mL^{-1} – 2500 ng mL^{-1}) with a limit of detection (LOD) of 0.033 pM (7.5 pg mL^{-1}) of MUC1. The proposed aptasensor offers acceptable selectivity, stability, and reproducibility in the determination of MUC1 spiked to human blood serum samples.

1. Introduction

Metal-organic frameworks (MOFs), as nano-scale porous materials, have attracted the attention of many researchers (Falcaro et al., 2016; Yang et al., 2017). Due to special properties of MOFs, including high surface area, high porosity and crystalline structure, their use in different fields, such as separation, sensing, catalysis, and gas adsorption, has been growing rapidly (Banerjee et al., 2015; Kaur et al., 2017; Shen et al., 2015; Wang et al., 2018).

MOFs are appropriate substrates for designing and manufacturing sensitive and selective electrochemical sensors (Lei et al., 2014; Liu and Yin, 2016; Morozan and Jaouen, 2012). However, due to drawbacks such as poor electrical conductivity and low mechanical stability of MOFs, their electrochemical applications are limited (Kreno et al., 2012; Liu et al., 2018).The composite of MOFs with other more conductive and mechanically stable materials, such as carbon nanostructures, is suggested as a solution to overcome the disadvantages of MOFs (Tran et al., 2017; Wang et al., 2016; Yang et al., 2015; Zhou et al., 2015).

Graphene has excellent electrical conductivity, high surface area, high chemical stability, and low cost which has widespread applications in the modification of electrodes (Chen et al., 2012; Song et al., 2016). Graphene can be combined with MOFs to achieve composite structures with desired electrical and chemical properties (Saraf et al., 2016; Yang et al., 2016).

In general, electrochemical biosensors can be divided to labeled and label-free ones (Han et al., 2010). Labeling process has disadvantages such as high cost, complexity, and changing biomolecule's activity. In label-free biosensors, on the other hand, an electroactive probe such as $[Fe(CN)_6]^{3-/4-}$ is added directly to the test solution (Kashefi-Kheyrabadi and Mehrgardi, 2012). This strategy may be associated with the undesirable accumulation of $[Fe(CN)_6]^{3-/4-}$ during the measurement. Another strategy is to modify the electrode surface by a substrate containing the electroactive species as a part of its structure (Amouzadeh Tabrizi et al., 2017). The electrochemical properties of this species should be changed as a response to the presence of target molecules, significantly. MOFs with numerous number of metallic centers in their crystalline structure may be used as proper electroactive substrates for electrode modification.

Mucin 1 (MUC1), a large glycoprotein, is expressed on the apical surface of most epithelial cells including mammary gland, gastrointestinal, respiratory, urinary and reproductive tracts (Hattrup and Gendler, 2008; S J Gendler and Spicer, 1995). In most of cancers, including colon, breast, ovarian, lung and pancreatic, MUC1 often becomes highly over expressed, so it is used as a cancer diagnostic marker (Henry and Hayes, 2012; Hollingsworth and Swanson, 2004; Ludwig

* Corresponding author.
E-mail addresses: fahimeh41@gmail.com, fjalali@razi.ac.ir (F. Jalali).

https://doi.org/10.1016/j.bios.2019.111433
Received 8 May 2019; Accepted 10 June 2019
Available online 11 June 2019
0956-5663/

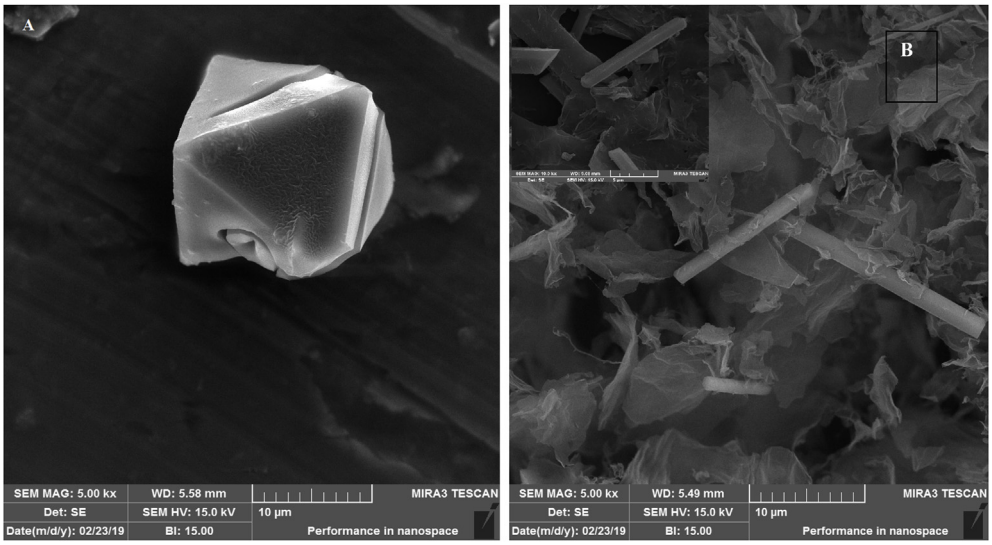

Fig. 1. SEM images of (A) cross-sectional view of Cu-MOF and (B) Cu-MOF-GO, **inset:**

and Weinstein, 2005).Therefore, developing a sensitive, simple and selective sensor for MUC1determination is very important.

In this work, for the first time, Cu^{2+} in a MOF structure (Cu-MOF) was used as an electrochemical probe for voltammetric detection of MUC1. To increase the conductivity of the electrode, electrochemically reduced graphene oxide (RGO) was added to Cu-MOF. Cu-MOF-RGO was a proper platform for aptamer immobilization on the electrode surface, as well. Due to the large amounts of copper in the Cu-MOF structure, a large anodic current was observed on aptamer/Cu-MOF-RGO electrode in phosphate buffer solution. It decreased significantly in MUC1 solution, which could be related to the formation of bulky aptamer-MUC1 adduct at the electrode surface, disturbing the electron transfer of Cu. The decreased anodic current was proportional to MUC1 concentration in solution.

2. Experimental

All chemicals were of analytical grade and prepared with double-distilled water. Trimesic acid (benzene-1,3,5-tricarboxylic acid, H_3BTC), copper nitrate hexahydrate Cu $(NO_3)_2.6H_2O$, 1- ethyl-3-(3-dimethylaminopropyl) carbodiimide (EDC) and N-hydroxysuccinimide (NHS) were purchased from Sigma-Aldrich. Graphite powder, N,N- dimethylformamide (DMF), potassium dihydrogen phosphate (KH_2PO_4) and potassium chloride (KCl) were obtained from Merck (Darmstadt, Germany). MUC1 and its specific oligonucleotide with the following sequence were prepared from Invitrogen (USA):

2.1. 5′-H_2N-$(CH_2)_6$- TTTTTACCCA GGGTGGGTGGG TGGGT-3′

All samples were dissolved in phosphate buffer solution, PBS (pH 7.4, 0.1 M) and stored in a refrigerator before use.

2.2. Apparatus

Cyclic voltammetry (CV), differential pulse voltammetry (DPV) and electrochemical impedance spectroscopy (EIS) were performed using a µ-Autolab electrochemical system equipped with NOVA1.10 software. In this work, a three-electrode system including modified glassy carbon electrode as a working electrode (3 mm in diameter)), Pt wire as auxiliary and Ag/AgCl (KCl, 3M) as reference electrodes was used. Morphological studies were proceed by TESCAN Mira 3 XMU field emission scanning electron microscope (FESEM, Czech Republic), with accelerating voltage at 15 kV and secondary electron (SE) as the detector. Fourier transform infra-red (FT-IR) spectra of products were recorded by using a Bruker spectrometer.

2.3. Preparation of Cu-MOF-GO nanocomposite

A solvothermal method was used for preparing the Cu-MOF based on a reported procedure (Chen et al., 2017). The procedure is illustrated in Supplementary File.

Graphene oxide (GO) was synthesized in our laboratory by modified Hummers method (Hummers and Offeman, 1958). Cu-MOF-GO nanocomposite was prepared by mixing Cu-MOF (1.0 mg) with GO (1.0 mg mL^{-1}) (Wang et al., 2014). The dispersion was then homogenized by ultrasonication for 1 h.

2.4. Fabrication of Cu-MOF-RGO/GCE

Cu-MOF-GO suspension (6 µL) was dropped onto the surface of a clean glassy carbon electrode (GCE) and dried at ambient temperature to obtain Cu-MOF-GO/GCE. Electrochemical reduction of GO was carried out by repetitive cyclic voltammetry (20 cycles) in the potential range of −1.5 to +0.6 V (against Ag/AgCl, KCl 3 M) in PBS (0.1 M, pH 7.4) at a scan rate of 0.05 V s^{-1} to obtain Cu-MOF-RGO/GCE. Immobilization of aminated aptamer of MUC1 on Cu-MOF-RGO/GCE was carried out by first, immersing in EDC (10 mM) and NHS (20 mM) solutions for 1 h. Then, the electrode was washed with PBS and incubated with MUC1 aptamer (1.0 µM in PBS) for 24 h at 4 °C. Finally, the electrode was thoroughly washed with double distilled water, and stored at 4 °C in PBS (0.1 M, pH 7.4) when not in use.

3. Results and discussion

3.1. Characterization of prepared Cu-MOF and Cu-MOF-GO powders

The morphology of nanocomposite was studied by FESEM. The octahedral crystals of Cu-MOF were obviously observed (Fig. 1A, cross section view). Fig. 1B shows that Cu-MOF nanocrystals were well distributed on GO sheets, while holding their original octahedral shape (inset: higher resolution of GO-Cu-MOF nanocomposite).

More investigation of nanocomposite structure was done by comparison of FT-IR spectra of GO, Cu-MOF and Cu-MOF-GO (Supplementary File, Fig. S1).

Electrochemical behavior of Cu-MOF-RGO/GCE was studied by cyclic voltammetry (in PBS, 0.1 M, pH 7.4) in a potential range of −1.0

to +1.0 V at a scan rate of 100 mV s^{-1} (Fig. S2). The redox peaks of Cu were largely increased in the presence of RGO.

Various potential scan rates were applied to the electrode in the range of 10–100 mVs^{-1} (Fig. S3), which proved a surface - confined redox process.

3.2. Characterization of different modified electrodes

FT-IR spectroscopy, EIS and CV methods were used to study the stepwise modification of electrode surface (Fig. S4), which confirmed the stable formation of aptamer/Cu-MOF-RGO/GCE.

3.3. Optimization of experimental conditions for electroanalysis of MUC1 on aptamer/Cu-MOF-RGO/GCE

Optimization of factors affecting the response of the aptasensor in the presence of MUC1 (1.0 pM) was investigated by differential pulse voltammetry, DPV. As the incubation time was increased, the current change (ΔI) of aptamer/Cu-MOF-RGO/GCE enhanced, gradually to 40 min incubation with MUC1 (Fig. S5). Longer contact times did not result in significant improvement in current, which could be due to the saturation of the electrode surface. The effect of solution pH (Fig. S5) was studied by recording DPV curves in MUC1 solution with different pH values. By increasing pH from 5.4 to 7.4, ΔI increased and then decreased at alkaline solutions, due to the optimized configuration and function of biological compounds at physiological pH 7.4. All the experiments were then performed in PBS (pH 7.4, 0.1 M).

Under optimized experimental conditions, CV curves were recorded in different concentrations of MUC1 (Supplementary File, Fig. S6), which showed continuous decrease of copper peaks in response to the presence of MUC1. The observation was assigned to the formation of MUC1-aptamer complex at the electrode surface which inhibited the redox reaction of copper in Cu-MOF structure.

The method of DPV was selected for sensitive determination of MUC1 by using aptamer/Cu-MOF-RGO/GCE as the working electrode. The oxidation peak current of copper decreased by adding more increments of MUC1 to the solution (Fig. 2). ΔI was proportional to the logarithm of MUC1 concentration ([MUC1]) from 0.1 pM to 10 nM (Inset). The regression equation was ΔI (μA) = 3 log [MUC1] (pM) + 0.1, with a squared correlation coefficient, R^2 = 0.993 and estimated limit of detection (LOD) of 0.03 pM.

In order to evaluate the usefulness of the prepared aptasensor in real sample analysis of MUC1, interference effect of some biological compounds was investigated (Fig. 3). The presence of 100 fold (compared to [MUC1] = 1.0 pM) ascorbic acid (AA), dopamine (D), glucose (G), vascular endothelial growth factor protein (VEGF165), Immunoglobulin G (IGG), bovine serum albumin (BSA) and human serum albumin (HSA) was tolerable and did not interfere in the determination of MUC1 by the proposed aptasensor.

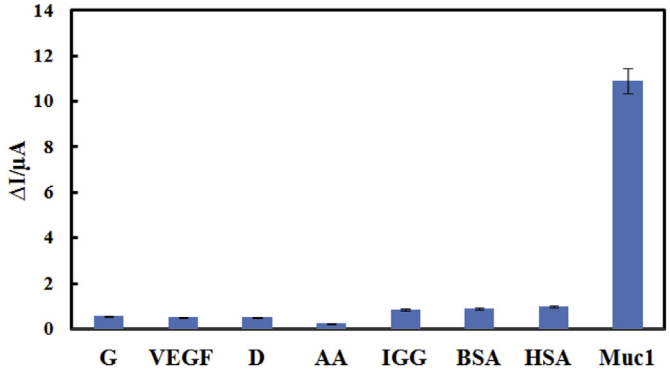

Fig. 3. Selectivity of the proposed aptasensor for MUC1 (1.0 pM) in presence of 100 times excess of ascorbic acid (AA), dopamine (D), glucose (G), vascular endothelial growth factor protein (VEGF165) Immunoglobulin G (IGG), bovine serum albumin (BSA) and human serum albumin (HSA).

The analytical figures of the proposed aptasensor were compared with some of the other biosensors reported for MUC1 (Table S1). It is clear that it has a better performance than most of the previous reported works. The simplicity and robustness of the nanocomposite (Cu-MOF-RGO), its good electrical conductivity and using the copper content of the Cu-MOF as the electrochemical probe, are significant.

To investigate the stability of aptamer/Cu-MOF-RGO/GCE, it was immersed in PBS (0.1 M, pH 7.4) and stored in refrigerator at 4 °C for 7 days, then it was used in the determination of MUC1 (1.0 pM) by the proposed method. The signal had only 5.81% drift compared to the freshly prepared electrode, suggesting acceptable stability.

The reproducibility of the method was studied by using 5 different electrodes modified with the same procedure. The relative standard deviation (RSD%) calculated as 5.33% for the determination of MUC1 (1.0 pM), which showed high reproducibility of aptasensor preparation.

The accuracy of the proposed method was evaluated by MUC1 determination in human blood serum samples. The standard addition method was used for measuring MUC1 in diluted blood samples (10 times). According to the results (Table S2), the proposed aptasensor exhibited acceptable recovery for MUC1 in real samples. Student t-test (for n = 3 at 95% confidence level, $t_{critical}$ = 4.3) was applied to the first data in Table S2 (average concentration of MUC1 from 3 replicate measurements, xbar), which was obtained before adding the standard

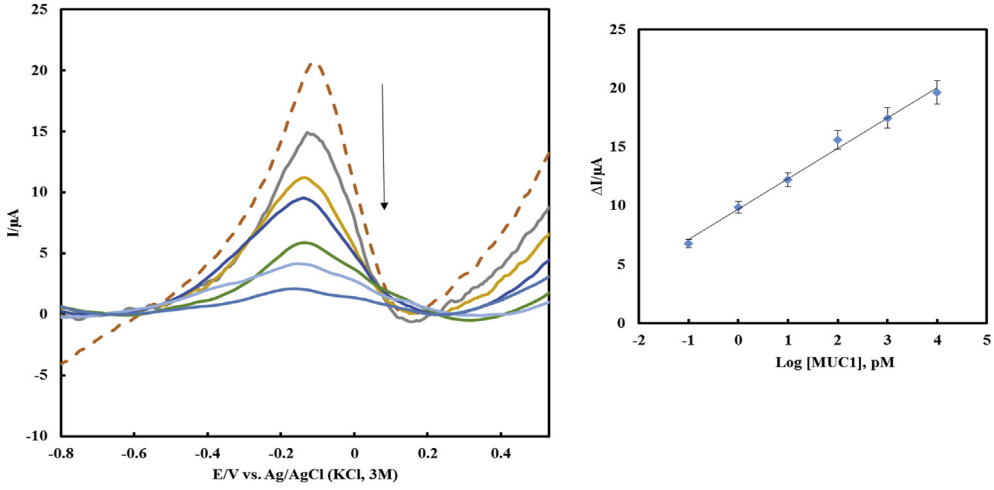

Fig. 2. DPV results for aptamer/Cu-MOF-RGO/GCE incubated with various concentrations of MUC1, (inset) calibration curve (ΔI_p versus log [MUC1].

solution to the blood serum sample. The calculated t (= xbar × √n/s) was much larger than $t_{critical}$, which means the presence of MUC1 in blood serum sample with a probability of 95%.

4. Conclusions

In this work, we showed the usefulness of electrode modification with Cu-MOF-RGO as an electrochemical probe in a new MUC1-aptasensor. The presence of RGO compensated for the weak conductivity of Cu-MOF. The modified electrode was characterized by SEM, FT-IR, and CV methods. After immobilization of the aptamer, the obtained aptasensor was used as one of the most sensitive electrochemical MUC1-biosensors. As the electrochemical probe, Cu present in the Cu-MOF structure responded to the presence of sub-picomolar levels of the tumor marker. The linear range obtained from DPV was 0.1 pM–10 nM (25 pg mL^{-1} – 2500 ng mL^{-1}) and the detection limit was 0.03 pM (7.5 pg mL^{-1}). The aptasensor was applied to the determination of MUC1 in human blood serum samples. The results indicated good accuracy and precision of the method. Compared with many previous methods, the construction of biosensors by using proper MOFs with highly ordered electroactive metallic centers is simpler, more straightforward and without need for additional redox probes.

Conflict of interest

We declare that we do not have any commercial or associative interest that represents a conflict of interest in connection with the work submitted.

Acknowledgments

Authors are greatly thankful of research council of Razi University for the financial support of the present work.

Appendix A. Supplementary data

Supplementary data to this article can be found online at https://doi.org/10.1016/j.bios.2019.111433.

References

Amouzadeh Tabrizi, M., Shamsipur, M., Saber, R., Sarkar, S., 2017. Sensor. Actuator. B Chem. 240, 1174–1181.
Banerjee, P.C., Lobo, D.E., Middag, R., Ng, W.K., Shaibani, M.E., Majumder, M., 2015. ACS Appl. Mater. Interfaces 7 (6), 3655–3664.
Chen, D., Feng, H., Li, J., 2012. Chem. Rev. 112 (11), 6027–6053.
Chen, Q., Li, X., Min, X., Cheng, D., Zhou, J., Li, Y., Xie, Z., Liu, P., Cai, W., Zhang, C., 2017. J. Electroanal. Chem. 789, 114–122.
Falcaro, P., Ricco, R., Yazdi, A., Imaz, I., Furukawa, S., Maspoch, D., Ameloot, R., Evans, J.D., Doonan, C.J., 2016. Coord. Chem. Rev. 307, 237–254.
Gendler, S.J., Spicer, A.P., 1995. Annu. Rev. Physiol. 57 (1), 607–634.
Han, K., Liang, Z., Zhou, N., 2010. Sensors 10 (5), 4541–4557.
Hattrup, C.L., Gendler, S.J., 2008. Annu. Rev. Physiol. 70 (1), 431–457.
Henry, N.L., Hayes, D.F., 2012. Mol. Oncol. 6 (2), 140–146.
Hollingsworth, M.A., Swanson, B.J., 2004. Nat. Rev. Canc. 4, 45.
Hummers, W.S., Offeman, R.E., 1958. JACS 80 (6) 1339-1339.
Kashefi-Kheyrabadi, L., Mehrgardi, M.A., 2012. Biosens. Bioelectron. 33 (1), 184–189.
Kaur, R., Sharma, A.L., Kim, K.-H., Deep, A., 2017. J. Ind. Eng. Chem. 53, 77–81.
Kreno, L.E., Leong, K., Farha, O.K., Allendorf, M., Van Duyne, R.P., Hupp, J.T., 2012. Chem. Rev. 112 (2), 1105–1125.
Lei, J., Qian, R., Ling, P., Cui, L., Ju, H., 2014. Trac. Trends Anal. Chem. 58, 71–78.
Liu, W., Yin, X.-B., 2016. Trac. Trends Anal. Chem. 75, 86–96.
Liu, L., Zhou, Y., Liu, S., Xu, M., 2018. ChemElectroChem 5 (1), 6–19.
Ludwig, J.A., Weinstein, J.N., 2005. Nat. Rev. Canc. 5, 845.
Morozan, A., Jaouen, F., 2012. Energy Environ. Sci. 5 (11), 9269–9290.
Saraf, M., Rajak, R., Mobin, S.M., 2016. J. Mater. Chem. 4 (42), 16432–16445.
Shen, W.-J., Zhuo, Y., Chai, Y.-Q., Yuan, R., 2015. Anal. Chem. 87 (22), 11345–11352.
Song, Y., Luo, Y., Zhu, C., Li, H., Du, D., Lin, Y., 2016. Biosens. Bioelectron. 76, 195–212.
Tran, T.Q.N., Das, G., Yoon, H.H., 2017. Sensor. Actuator. B Chem. 243, 78–83.
Wang, X., Wang, Q., Wang, Q., Gao, F., Gao, F., Yang, Y., Guo, H., 2014. ACS Appl. Mater. Interfaces 6 (14), 11573–11580.
Wang, M.-Q., Zhang, Y., Bao, S.-J., Yu, Y.-N., Ye, C., 2016. Electrochim. Acta 190, 365–370.
Wang, M., Guo, L., Cao, D., 2018. Anal. Chem. 90 (5), 3608–3614.
Yang, J., Zhao, F., Zeng, B., 2015. RSC Adv. 5 (28), 22060–22065.
Yang, Y., Wang, Q., Qiu, W., Guo, H., Gao, F., 2016. J. Phys. Chem. C 120 (18), 9794–9803.
Yang, Q., Xu, Q., Jiang, H.-L., 2017. Chem. Soc. Rev. 46 (15), 4774–4808.
Zhou, J., Li, X., Yang, L., Yan, S., Wang, M., Cheng, D., Chen, Q., Dong, Y., Liu, P., Cai, W., Zhang, C., 2015. Anal. Chim. Acta 899, 57–65.